A MIR17HG-derived Long Noncoding RNA Provides an Essential Chromatin Scaffold for Protein Interaction and Myeloma Growth

American Society of Hematology
2021 L Street NW, Suite 900,
Washington, DC 20036
Phone: 202-776-0544 | Fax 202-776-0545
editorial@hematology.org

A MIR17HG-derived Long Noncoding RNA Provides an Essential Chromatin Scaffold for Protein Interaction and Myeloma Growth

Tracking no: BLD-2022-016892R2

Eugenio Morelli (Dana Farber Cancer Institute, United States) Mariateresa Fulciniti (Dana Farber Cancer Institute, United States) Mehmet Samur (Dana-Farber Cancer Institute and Harvard School of Public Health, United States) Caroline Ribeiro (Weill Cornell Medical College, United States) Leon Wert-Lamas (Dana Farber Cancer Institute, United States) Jonathan Henninger (Whitehead Institute of Biomedical Research, United States) Annamaria Gulla (Dana-Farber Cancer Institute, United States) Anil Aktas Samur (Dana Farber Cancer Institution, United States) Katia Todoerti (Fondazione Cà Granda IRCCS Policlinico, Italy) Srikanth Talluri (DFCI, United States) Woojun Park (Baylor College of Medicine, United States) Cinzia Federico (ASST DEGLI SPEDALI CIVILI DI BRESCIA, Italy) Francesca Scionti (Institute for Biomedical Research and Innovation (IRIB), National Research Council of Italy (CNR), 98164 Messina, Italy, Italy) Nicola Amodio (University Magna Graecia of Catanzaro, Italy) Giada Bianchi (Brigham and Women's Hospital, United States) Megan Johnstone (Dana Farber Cancer Institute, United States) Na Liu (Dana Farber Cancer Institute, United States) Doriana Gramegna (Dana Farber Cancer Institute, United States) Domenico Maisano (Dana-Farber Cancer Institute, United States) Nicola Russo (Biogem s.c.ar.l,, Italy) Charles Lin (Baylor College of Medicine, United States) Yu-Tzu Tai (Dana Farber Cancer Institute, United States) Antonino Neri (University of Milan, Italy) Dharminder Chauhan (Dana Farber Cancer Institute, United States) Teru Hideshima (Dana-Farber Cancer Institute, United States) Masood Shammas (Dana Farber Cancer Institute, United States) Pierfrancesco Tassone (Magna Graecia University, Italy) Sergei Gryaznov (MAIA Therapeutics, United States) Richard Young (Whitehead Institute, United States) Kenneth Anderson (Dana Farber Cancer Institute, United States) Carl Novina (Harvard Medical School, United States) Massimo Loda (Weill Cornell Medicine, United States) Nikhil Munshi (V/A healthcare system, United States)

Abstract:
Long noncoding RNAs (lncRNA) can drive tumorigenesis and are susceptible to therapeutic intervention. Here, we used a large-scale CRISPR *interference* viability screen to interrogate cell growth dependency to lncRNA genes in multiple myeloma (MM), and identified a prominent role for the *miR-17-92 cluster host gene* (MIR17HG). We show that a MIR17HG-derived lncRNA, named lnc-17-92, is the main mediator of cell growth dependency acting in a microRNA- and DROSHA- independent manner. Lnc-17-92 provides a chromatin scaffold for the functional interaction between c-MYC and WDR82, thus promoting the expression of *ACACA*, which encodes the rate-limiting enzyme of *de novo* lipogenesis acetyl-coA carboxylase 1 (ACC1). Targeting MIR17HG pre-RNA with clinically applicable antisense molecules disrupts the transcriptional and functional activities of lnc-17-92, causing potent anti-tumor effects both *in vitro* and *in vivo* in three pre-clinical animal models, including a clinically relevant PDX-NSG mouse model. This study establishes a novel oncogenic function of MIR17HG and provides potent inhibitors for translation to clinical trials.

Conflict of interest: COI declared - see note

COI notes: N.C.M. serves on advisory boards/consultant to Takeda, BMS, Celgene, Janssen, Amgen, AbbVie, Oncopep, Karyopharm, Adaptive Biotechnology, and Novartis and holds equity ownership in Oncopep. K.C.A. serves on advisory boards to Janssen, Pfizer, Astrazeneca, Amgen, Precision Biosciences, Mana, Starton, and Raqia, and is a Scientific Founder of OncoPep and C4 Therapeutics. R.A.Y. is a founder and shareholder of Syros Pharmaceuticals, Camp4 Therapeutics, Omega Therapeutics, and Dewpoint Therapeutics. E.M., S.G. and N.C.M filed a provisional patent on MIR17HG as a target for cancer therapy. No potential conflicts of interest were disclosed by the other authors. D.C. reports other support from Stemline Therapeutics, Oncopeptides, and C4 Therapeutics outside the submitted work.

Preprint server: Yes; Biorxiv https://doi.org/10.1101/2021.12.08.471297

Author contributions and disclosures: E.M. and N.C.M. conceived and designed the research studies. E.M., M.F. and N.C.M. wrote the manuscript. M.K.S., A.A.S. and K.T. performed in silico analysis of transcriptomic data. C.F.R. performed lipidomic studies. L.W.L. performed yeast-3-hybrid experiments. J.E.H. performed RNA FISH, dual RNA FISH and Co-IF/dual RNA FISH. S.T. provided MM cells expressing CAS9. W.D.P. analyzed ChIP-seq data. S.G. designed t-ASOs. C.F., N.R. and F.S. provided support for the identification of RROL isoforms. M.F., A.G., N.A., M.J., G.B., C.L., Y.T.T., A.N., D.C., T.H., M.A.S., P.T., R.A.Y., K.C.A., C.D.N. and M.L. contributed to the design and interpretation of key experiments. M.L. supervised lipidomic studies. C.D.N. supervised Y3H experiments.

Non-author contributions and disclosures: Yes; We thank Dr. Christina Usher (Dana-Farber Cancer Institute) for editing the manuscript and insightful comments.

Agreement to Share Publication-Related Data and Data Sharing Statement: RNA-seq data after depletion of lnc-17-92 have been deposited and are publicly available.

Clinical trial registration information (if any):

A MIR17HG-derived Long Noncoding RNA Provides an Essential Chromatin Scaffold for Protein Interaction and Myeloma Growth

Short title: A long noncoding RNA supporting myeloma.

Eugenio Morelli[1,2,*], Mariateresa Fulciniti[1,2], Mehmet K. Samur[1,2], Caroline F. Ribeiro[3], Leon Wert-Lamas[4], Jon E. Henninger[5], Annamaria Gullà[1,2], Anil Aktas-Samur[1,2], Katia Todoerti[6], Srikanth Talluri[1,2,7], Woojun D. Park[8], Cinzia Federico[9], Francesca Scionti[14], Nicola Amodio[9], Giada Bianchi[1,2], Megan Johnstone[1], Na Liu[1], Doriana Gramegna[1,2], Domenico Maisano[1,2], Nicola A. Russo[10], Charles Lin[8], Yu-Tzu Tai[1,2], Antonino Neri[6,11,12], Dharminder Chauhan[1,2], Teru Hideshima[1,2], Masood A. Shammas[1,2,7], Pierfrancesco Tassone[9], Sergei Gryaznov[13], Richard A. Young[5], Kenneth C. Anderson[1,2], Carl D. Novina[4], Massimo Loda[3], and Nikhil C. Munshi[1,2,7,*].

[1]Department of Medical Oncology, Jerome Lipper Multiple Myeloma Center; Dana-Farber Cancer Institute; Boston, MA, 02215; USA.

[2]Harvard Medical School, Boston, MA, 02215; USA.

[3]Department of Pathology and Laboratory Medicine; Weill Cornell Medical College; New York, NY, 10065; USA.

[4]Department of Cancer Immunology and Virology; Dana-Farber Cancer Institute; Boston, MA, 02215; USA.

[5]Whitehead Institute of Biomedical Research; Massachusetts Institute of Technology; Cambridge, MA, 02142; USA.

[6]Department of Hematology; Fondazione Cà Granda IRCCS Policlinico; Milan, 20122; Italy.

[7]VA Boston Healthcare System; Boston, MA, 02132; USA.

[8]Department of Molecular and Human Genetics; Baylor College of Medicine; Houston, TX, 77030; USA.

[9]ASST DEGLI SPEDALI CIVILI DI BRESCIA, Italy.

[10]Istituto di Ricerche Genetiche "G. Salvatore"; Biogem s.c.ar.l,; Avellino, 83031; Italy.

[11]Department of Oncology and Hemato-oncology; University of Milan; Milan, 20122; Italy.

[12]Scientific Directorate, Azienda USL-IRCCS Reggio Emilia, 42123, Italy

[13]Maia Biotechnology Inc, 444 W. Lake St., STE 1700, Chicago, IL 60606.

[14]Institute for Biomedical Research and Innovation (IRIB)

[*]Correspondence: Nikhil_munshi@dfci.harvard.edu; Eugenio_morelli@dfci.harvard.edu.

Word counts (text): 3887

Word counts (abstract): 152

Figures: 6

References: 67

KEY POINTS

- MIR17HG produces a long noncoding RNA that acts as a chromatin scaffold for protein interaction and tumor cell growth.
- Targeting this long noncoding RNA with optimized antisense oligonucleotides has potent anti-myeloma activity in pre-clinical models.

ABSTRACT

Long noncoding RNAs (lncRNA) can drive tumorigenesis and are susceptible to therapeutic intervention. Here, we used a large-scale CRISPR *interference* viability screen to interrogate cell growth dependency to lncRNA genes in multiple myeloma (MM), and identified a prominent role for the *miR-17-92 cluster host gene* (MIR17HG). We show that a MIR17HG-derived lncRNA, named lnc-17-92, is the main mediator of cell growth dependency acting in a microRNA- and DROSHA- independent manner. Lnc-17-92 provides a chromatin scaffold for the functional interaction between c-MYC and WDR82, thus promoting the expression of *ACACA*, which encodes the rate-limiting enzyme of *de novo* lipogenesis acetyl-coA carboxylase 1 (ACC1). Targeting MIR17HG pre-RNA with clinically applicable antisense molecules disrupts the transcriptional and functional activities of lnc-17-92, causing potent anti-tumor effects both *in vitro* and *in vivo* in three pre-clinical animal models, including a clinically relevant PDX-NSG mouse model. This study establishes a novel oncogenic function of MIR17HG and provides potent inhibitors for translation to clinical trials.

INTRODUCTION

Multiple myeloma (MM) is a genetically complex malignancy of plasma cells that accounts for about 10% of hematologic cancers and remains largely incurable[1]. A growing body of evidence points to a key role played by noncoding RNA (ncRNA) networks in MM[2], suggesting that MM cells can become significantly addicted to and therapeutically susceptible to the modulation of oncogenic ncRNAs[3-8]. In particular, long ncRNAs (lncRNAs) outnumber protein-coding genes in humans and are susceptible to the same oncogenic pathogenetic events[9,10]. These RNA molecules, defined as transcripts greater than 200nt with no protein-coding potential, have a diverse array of functional roles, ranging from being precursor molecules for the biogenesis of mature microRNAs (miRNAs) to direct interactions with proteins and nucleic acids to regulate protein function and/or stability[11-13]. With the plethora of biological functions that lncRNAs modulate to control cellular processes at multiple levels, it is not surprising that their aberrant expression and function have been implicated in the progressive gain of a malignant phenotype by tumor cells[14]. Indeed, the expression of 14 lncRNAs in newly diagnosed MM patients is correlated (or anti-correlated) with progression-free survival independent of cytogenetic, international staging system (ISS), or minimal residual disease (MRD) status[15]. Other lncRNAs, including SMILO, also independently predict MM progression and response to therapy[16,17].

To find lncRNAs that have a direct impact on MM proliferation and survival, thus providing cell growth dependency, we conducted a lncRNA-targeted large-scale CRISPR *interference* (CRISPRi) viability screen. CRISPRi makes use of a catalitically inactive Cas9 (dCas9)-KRAB fusion protein to repress the expression of endogenous

lncRNA genes[18,19]. From this screen, we identified MIR17HG as essential in MM and *i*) characterized its novel function as lncRNA mediating protein-protein and protein-DNA interactions, *ii*) developed potent inhibitors for translation to clinical trials.

METHODS

Cells

Human cell lines and primary cells were grown at 37°C, 5% CO_2. Detailed information is included in Supplementary Methods section.

RNA-seq, microarray-based gene expression analysis and miRNA profiling of MM patients and cell lines.

These analyses were performed in purified CD138+ cells. Detailed information can be found in Supplementary Methods section.

CRISPRi viability screen and validation

Cell lines expressing the dCas9-KRAB fusion protein were generated as previously described[19]. Detailed information on library design, gRNA pool library production, titering of virus, primary and secondary screenings, validation study, as well as on data analysis can be found in Supplementary Methods section.

Antisense oligonucleotides (ASO), synthetic miRNA mimics and inhibitors, siRNAs

Long Non-Coding LNA gapmerRs were custom-designed and purchased from Exiqon (Vedbaek, Denmark). Sequences can be found in Supplementary Methods section. Synthetic miRNA mimics and inhibitors, as well as silencer select siRNAs, were purchased from Ambion (Applied Biosystems, CA, US). SiRNA pool targeting WDR82 was purchased from Horizon Discovery (Waterbeach, U.K.). Design of clinically applicable ASOs is described in **Supplementary Table 8**.

Gymnosis

Gymonotic experiments were performed as previously described[20].

Transient and stable transfection of cells

Cell transfection and transduction was performed as previously described[5]. Detailed information can be found in Supplementary Methods section.

Detection of cell proliferation and apoptosis.

Cell viability was evaluated by Cell Counting Kit-8 (CCK-8) assay (Dojindo Molecular Technologies), according to the manufacturer's instructions. Apoptosis was investigated by an Annexin V/7-AAD flow cytometry assay using FACS CANTO II (BD Biosciences).

Reverse transcription (RT) and quantitative real-time amplification (qRT-PCR)

RNA extraction, reverse transcription (RT) and quantitative real-time amplification (qRT-PCR) were performed as previously described[5]. Detailed information can be found in Supplementary Methods section.

Western blot analysis

Protein extraction and western blot analysis were performed as previously described. Detailed information can be found in Supplementary Methods section.

RNA FISH and Co-immunofluorescence with RNA FISH (Co-IF/FISH)

These experiments were conducted according to established protocols[21,22]. Detailed information can be found in Supplementary Methods section.

Luciferase reporter assay

Promoter reporter clones for human *ACACA* (NM_198834), *ANO6* (NM_001025356), *CCDC91* (NM_018318), *EPT1* (NM_033505), *EXT1* (NM_000127), *FER* (NM_001308028) and *ZYG11A* (NM_001004339) were cloned into the GLuc-ON™ Promoter Reporter Vector (GeneCopoeia, Rockville, MD). A luciferase reporter assay was performed according to the manufacturer's instructions.

ChIRP

Lnc-17-92 and LacZ antisense DNA probes were designed using the online probe designer at singlemoleculefish.com. Oligonucleotides were biotinylated at the 3′ end with an 18-carbon spacer arm. AMO1 cells were collected and subjected to ChIRP using the EZ- Magna ChIRP RNA Interactome Kit (Millipore Sigma, Bedford, MA), according to the manufacturer's instructions and established protocols[23].

***De novo* lipogenesis assay**

These experiments were conducted as previously described[24]. Detailed information can be found in Supplementary Methods section.

ChIP-qPCR

ChIP-qPCR was performed as previously described[25]. Detailed information can be found in Supplementary Methods section.

RNA-Protein Pull-Down

Lnc-17-92 transcripts and truncated versions were cloned into a pBlueScript vector and sequence verified. In vitro transcription and biotinylation was performed using AmpliScribe™ T7-Flash™ Biotin-RNA Transcription Kit (Lucigen, cat. no. #ASB71110), according to the manufacturer's instructions. Cell nuclear lysates (from $1x10^7$ AMO1 cells) were incubated with biotinylated RNA and streptavidin beads for RNA pull-down incubation, using Pierce™ Magnetic RNA-Protein Pull-Down Kit (Thermo Fisher Scientific, cat. no. #20164), according to the manufacturer's instructions. RNA-associated proteins were eluted and analyzed by western blotting.

RNA Yeast 3 Hybrid

These experiments were conducted according to established protocols[21,22]. Detailed information can be found in Supplementary Methods section.

RIP-qPCR

RNA immunoprecipitation (RIP) experiments were performed using the Magna RIP RNA-binding Protein Immunoprecipitation Kit (Millipore Sigma, cat. no. 17-701), according to the manufacturer's instructions. The anti-MYC antibody [Y69] used for RIP was purchased from Abcam (ab32072). Normal Rabbit IgG was purchased from Cell

Signaling Technology (cat. no. #2729). The primers used for detecting lnc-17-92 are listed in Supplementary Methods section.

Co-immunoprecipitation (Co-IP)

Protein lysates were obtained from $1x10^7$ cells (AMO1, H929 and $U266^{MYC+}$, with corresponding treatments). Coimmunoprecipitation was performed using the Pierce™ Co-Immunoprecipitation Kit (Thermo Fisher Scientific, cat. no. 26149), according to the manufacturer's instructions. IP antibodies are listed in Supplementary Methods section.

Proximity-dependent biotin identification (BioID)

BioID was performed as described by Kalkat *et al.*[26]. Detailed information can be found in Supplementary Methods section.

Mass Spectrometry

Mass Spectrometry analysis of Co-IP and BioID samples was performed at the Taplin Mass Spectrometry Facility (Harvard Medical School, Boston, MA).

Animal study

6-week-old female immunodeficient NOD.CB17-Prkdcscid/NCrCrl (NOD/SCID) mice (Charles River) or NSG mice (Jackson Laboratory) were housed in our animal facility at Dana-Farber Cancer Institute (DFCI). All experiments were performed after approval by the Animal Ethics Committee of the DFCI and performed using institutional guidelines. Detailed information can be found in Supplementary Methods section.

198

199 **Statistical Analysis**

200 All *in vitro* experiments were repeated at least three times and performed in triplicate. A
201 representative experiment was shown in the figures. Statistical significances of
202 differences were determined using Student's t test (unless otherwise specified), with the
203 minimal level of significance specified as $p<0.05$. Kaplan-Meier survival curves were
204 compared by log-rank test. Statistical analyses were determined using GraphPad
205 software (http://www.graphpad.com). Graphs were obtained using GraphPad software
206 (unless otherwise specified).

207

208 **Data availability**

209 The authors declare that all data supporting the findings of this study are available
210 within the article and its Supplementary Information. Files or reagents are available from
211 the corresponding authors on request. Data is stored at accession number GSE208599.

RESULTS

CRISPRi viability screens identify MIR17HG as a leading cell growth dependency in MM.

We analyzed RNA-seq data from 360 newly diagnosed MM patients and identified 913 lncRNA transcripts expressed in primary MM cells (**Fig. 1A, I.**) and in a panel of 70 MM cell lines (data not shown). To systematically interrogate the role of these lncRNAs in MM cell growth, we transduced 3 MM cell lines (H929, KMS-11 and KMS-12-BM) engineered to express a dCAS9-KRAB fusion protein with a pooled library consisting of 7 sgRNAs against each of the 913 transcription start sites (TSS) of the identified lncRNAs and 576 negative control sgRNAs (**Fig. 1A, II.** and **Supplementary Table 1**). After 3 weeks, we tested for sgRNAs that were relatively depleted or enriched in the MM cell population using deep sequencing and the Model-based Analysis of Genome-wide CRISPR-Cas9 Knockout (MAGeCK) robust rank aggregation (RRA) algorithm[27].

The most enriched or depleted sgRNAs were further tested in secondary screens using a pooled library targeting the TSS of 224 lncRNAs, the TSS of known protein-coding oncogenes (MYC, IRF4)[28,29] or tumor suppressors (TP53)[30] as positive controls, and 2245 non-targeting sgRNAs as negative controls (**Fig. 1A; III.** and **Supplementary Table 2)**. In the secondary screens, 4 MM cell lines (H929, KMS11, KMS12BM and AMO1) were used to detect and rank significantly depleted or enriched sgRNAs. As expected, sgRNAs targeting IRF4 and MYC were significantly depleted in three (MYC) or all (IRF4) cell lines, while sgRNAs targeting TP53 were significantly enriched in both TP53 wild-type cell lines (AMO1 and H929)[31].

Focusing on depleted sgRNAs, we identified lncRNA dependencies in MM cells that were either cell-line specific (54%) or shared (46%) **(Supplementary Fig. 1A** and **Supplementary Table 3).** A ranked analysis of sgRNA depletion identified MIR17HG as the leading dependency, with RRA scores equal or superior to those obtained by targeting MYC or IRF4 in all cell lines tested (**Fig.1B)**. To validate this data further, we next transduced MM cell lines expressing dCAS9-KRAB fusion protein with the top four sgRNAs targeting MIR17HG under the regulation of a tetracycline-inducible promoter and observed reduced cell growth compared to cells infected with non-targeting sgRNAs after continued exposure to doxycycline (**Fig. 1C** and **Supplementary Fig. 1B**). Moreover, we used 2 different locked nucleic acid (LNA) gapmeR ASOs (simply referred to as ASO), which target the MIR17HG nascent RNA (pre-RNA) for RNase H–mediated degradation[32,33], to transfect 11 MM cell lines including those resistant to conventional anti-MM agents (AMO1-ABZB resistant to bortezomib; AMO1-ACFZ resistant to carfilzomib; MM.1R resistant to dexamethasone) and confirmed a significant impact on MM cell viability independent of the genetic and molecular background (**Fig. 1D** and **Supplementary Fig. 1C**).

MIR17HG-derived lnc-17-92 mediates cell growth dependency in a miRNA- and DROSHA-independent manner.

MIR17HG is the locus of the miRNA cluster miR-17-92 and a lncRNA[34,35], named here lnc-17-92. Lnc-17-92 has two isoforms, one that is ~5,000 nt long (lnc-17-92^{TV1}) and one that is ~900 nt (lnc-17-92^{TV2})[34,35], and both have yet to be functionally explored (**Fig. 2A**). In MM cells, both RNA-seq (**Supplementary Fig. 2A)** and qRT-PCR

(**Supplementary Fig. 2B)** indicated preferential expression of lnc-17-92^{TV1}, which is the isoform further investigated in this study and hereafter referred to as lnc-17-92. Using RNA-seq, we confirmed its expression in CD138+ cells from an additional large cohort of MM patients (MMRF/CoMMpass, n=720) and in MM cell lines (n=60) (**Supplementary Fig. 2C-D**). In MM cell lines, we also demonstrated nuclear enrichment of lnc-17-92 using single molecule RNA-FISH (**Fig. 2B**) and subcellular qRT-PCR (**Supplementary Fig. 2E**). We observed that lnc-17-92 expression was higher during disease progression in two independent datasets from MM patients analyzed at diagnosis and/or relapse (**Supplementary Fig. 2F-G**) and that higher expression of lnc-17-92 was associated with shorter event-free survival (EFS) and overall (OS) survival in 3 large cohorts of newly diagnosed MM patients (**Fig. 2C**). Expression of lnc-17-92 did not significantly correlate with the expression of miR-17-92 miRNAs in CD138+ MM cells from 140 patients (average Spearman r = 0.16), suggesting that lnc-17-92 and miR-17-92 are under independent regulatory control and function in distinct molecular pathways mediating cell growth dependency to MIR17HG (**Supplementary Fig. 2H**).

To test independent activity of lnc-17-92, we first established two MM cell lines over-expressing miR-17-92 via ectopic expression of the primary precursor pri-mir-17-92 (**Supplementary Fig. 3A**). We specifically depleted lnc-17-92 in these cell lines with ASOs targeting the 5'-end of MIR17HG pre-RNA, a region not covered by pri-mir-17-92, and observed a significant inhibition of cell growth that was not rescued by ectopic pri-mir-17-92 (**Fig. 2D**). Next, we established two DROSHA knockout (DR-KO) MM cell lines (AMO1^{DR-KO} and H929^{DR-KO}), which are unable to enzymatically digest pri-mir-17-

92 and produce miR-17-92s (**Supplementary Fig. 3B**)[36], and still observed strong anti-proliferative activity in both DR-WT and DR-KO cell systems after lnc-17-92 depletion using gymnotic treatment with ASO1 (**Fig. 2E)** or after transfection with 3 different ASOs (-1/-2/-3) (**Supplementary Fig. 3C**). Importantly, exposure to gymnotic ASO1 (**Fig. 2E-F**) or transfection with ASO2 (**Supplementary Fig. 3D)** abrogated the ability of AMO1^{DR-KO} cells to establish tumors in NOD SCID mice, resulting in prolonged animal survival. Next, using the easy-to-transfect colorectal cancer cell line HCT-116, which is driven by MIR17HG[34], we found that ectopic expression of lnc-17-92^{TV1} significantly rescued the anti-proliferative activity of ASOs targeting MIR17HG pre-RNA more effectively than ectopic lnc-17-92^{TV2} or pri-mir-17-92 (**Supplementary Fig. 3E-F**). Finally, we confirmed the independent activity of lnc-17-92 in the HCT-116 and DLD-1 colorectal cancer cell lines carrying a mutant Dicer, which confers a hypo-morphic phenotype preventing the cells from enzymatically processing mature miRNAs[37] (**Supplementary Fig. 3G**).

These results indicate that lnc-17-92^{TV1} is the main mediator of MIR17HG cancer dependency, separate from the actions and biogenesis pathway of miR-17-92.

Lnc-17-92 forms a transcriptional axis with *ACACA* to promote MM cell growth.

The nuclear enrichment of lnc-17-92 suggests a possible role in the regulation of gene expression. We therefore depleted lnc-17-92 in DR-WT (AMO1 and H929) and DR-KO (AMO1^{DR-KO}) MM cell lines using early exposure to gymnotic ASO1 to avoid modulation of miR-17-92 (**Supplementary Fig. 4A**) and miR-17-92's canonical targets in DROSHA WT cells (**Supplementary Fig. 4B-C**) and identified 7 genes rapidly downregulated

after depletion of lnc-17-92 in all the cell lines tested (**Fig. 3A**). We validated these findings in CD138+ cells from 3 MM patients treated *ex-vivo* with ASO1 (**Fig. 3B**) and in the lymphoma cell lines Raji and Daudi (**Supplementary Fig. 4D**). Conversely, the expression of these genes was not affected by modulating individual members of miR-17-92 using synthetic mimics or inhibitors (**Supplementary Fig. 4E-F**). Moreover, we observed significant positive correlation (Spearman $r > 0.3$; $p<0.001$) between lnc-17-92 and its target genes in at least 1 out of 2 large RNA-seq MM patient datasets (IFM/DFCI and MMRF/CoMMpass) (**Fig. 3C**).

Using a luciferase reporter assay, performed in $293T^{DR\text{-}KO}$ cells in the presence or absence of lnc-17-92 depletion, we demonstrated that the regulatory control of lnc-17-92 over these genes, except *ANO6*, occurs at the promoter level (**Fig. 3D**). Consistently, we confirmed lnc-17-92 interaction at the promoter region of the top target, *ACACA*, by a chromatin isolation by RNA precipitation (ChIRP) assay followed by qRT-PCR analysis (**Fig. 3E** and **Supplementary Fig. 4G-H**) and showed frequent localization of lnc-17-92 to the *ACACA* locus by single-molecule dual RNA FISH analysis of lnc-17-92 and *ACACA* pre-mRNA (<300nm to nearest lnc-17-92 spot in ~50% of *ACACA* pre-RNA spots analyzed (n=60)) (**Fig. 3F**). Proximal localization of lnc-17-92 to the *ACACA* gene locus was significantly more frequent compared to random spots (**Fig. 3F**).

Among the identified lnc-17-92 targets, *ACACA* had the largest impact on the proliferation and survival of MM cells (**Fig. 3G**). *ACACA* encodes the rate-limiting enzyme for the *de novo* lipogenesis pathway ACC1, which supports tumorigenesis in different cancer contexts[38]. To confirm that lnc-17-92's control over *ACACA* expression

has a functional effect, we depleted lnc-17-92 and found that the incorporation of C^{14}-radiolabeled glucose into the lipid pool was significantly reduced, indicating a reduced amount of *de novo* lipogenesis[24], both in MM cell lines and CD138+ MM patient cells (**Supplementary Fig. 4I)**. This was not observed after transfection of MM cells with synthetic inhibitors of miR-17-92s (**Supplementary Fig. 4J)**. Moreover, supplementing palmitate, which is the main downstream product of ACC1 activity, significantly rescued the anti-proliferative and pro-apoptotic effects of lnc-17-92 depletion in MM cells (**Supplementary Fig. 4K-L**).

Altogether, these data indicate lnc-17-92 is a chromatin-interacting lncRNA with transcriptional regulatory functions. We next sought to determine how it can promote transcription by searching for its protein-binding partners.

Lnc-17-92 directly interacts with c-MYC and promotes its occupancy at the *ACACA* promoter.

The targeting of MIR17HG primarily kills c-MYC positive (MYC+) tumor cells, including in MM[5,34,39,40]. Intriguingly, MYC is known to reactivate *ACACA* expression and *de novo* lipogenesis in tumor cells[41], with MYC+ tumor cells becoming addicted to this metabolic pathway, findings that we validated in MM cells (**Supplementary Fig. 5A-D**). Therefore, we hypothesized that lnc-17-92 mediates the functional interplay between MYC and MIR17HG by directly interacting with MYC protein to promote gene expression.

We performed an RNA Protein pull-down (RPPD) experiment and found that MYC forms a complex with lnc-17-92^{TV1} (**Fig. 4A**). RNA immunoprecipitation (RIP) assay with MYC antibody confirmed the enrichment of lnc-17-92^{TV1} (**Fig. 4B**).

Moreover, an RNA yeast-3-hybrid (Y3H) assay confirmed the lnc-17-92^{TV1}-MYC interaction in an *in vivo* cellular model[42], as shown by yeast colony growth (**Fig. 4C**). An analysis using truncated versions of lnc-17-92^{TV1} further indicated the 3'-end regions, which do not include miR-17-92, as particularly relevant for the interaction with MYC in MM cells (**Supplementary Fig. 5E**).

Next, we evaluated if MYC and lnc-17-92 cooperate to promote *ACACA* expression in MM cells. Depletion of lnc-17-92 in MM cells indeed abrogated MYC occupancy at the *ACACA* promoter while not affecting MYC expression (**Fig. 4D**) and reduced the expression of *ACACA* in the conditional MYC Tet-Off cell line P493-6[43] only in presence of high MYC levels (**Fig. 4E**). Moreover, by coupling RNA FISH analysis of lnc-17-92^{TV1} and *ACACA* pre-RNA with immunofluorescence analysis of MYC protein (FISH/IF), we captured the co-localization of lnc-17-92^{TV1} and MYC at the *ACACA* gene locus (**Supplementary Fig. 5F**).

These data demonstrate that lnc-17-92^{TV1} forms an RNA-protein complex with the transcription factor MYC to promote its chromatin occupancy and transcriptional activity at the *ACACA* promoter.

Lnc-17-92 mediates the assembly of a MYC-WDR82 transcriptional complex, leading to transcriptional and epigenetic activation of *ACACA*.

MYC transcriptional activity is modulated through the interaction with transcriptional and epigenetic co-regulators[41]. To determine if lnc-17-92 affects these protein-protein interactions, we integrated the results of a proximity-dependent biotin identification (BioID) analysis (**Supplementary Fig. 6A**) with a co-immunoprecipitation assay

372 followed by mass-spectrometry analysis (Co-IP/MS) in three MM cell lines (AMO1,
373 H929 and U266^{MYC+}), in the presence and absence of depletion of lnc-17-92. This
374 analysis highlighted WDR82 as a very high-confidence lnc-17-92-dependent MYC
375 interactor (**Fig. 5A** and **Supplementary Tables 4-7**). A direct RNA-protein interaction
376 between lnc-17-92^{TV1} and WDR82 was further confirmed by both RPPD (**Fig. 5B**) and
377 RNA Y3H (**Fig. 5C**) assays. Analysis using the truncated versions of lnc-17-92^{TV1}
378 indicated that this interaction may involve different domains across lnc-17-92
379 (**Supplementary Fig. 6B**).

380 WDR82 is a regulatory component of the SET1 methyltransferase complex,
381 which catalyzes histone H3 Lys-4 (H3K4) methylation (mono-, di-, tri-) at the
382 transcriptional start sites of active loci[44,45], a prerequisite for MYC binding to chromatin
383 and transactivation[46]. We confirmed a global effect of silencing of WDR82 on H3K4
384 methylation in MM cells (**Supplementary Fig. 6C**). Consistently, depletion of WDR82
385 reduced the occupancy of H3K4me3 (**Fig. 5D** and **Supplementary Fig. 6D**) and MYC
386 (**Fig. 5E** and **Supplementary Fig. 6E**) at the *ACACA* promoter, and decreased *ACACA*
387 mRNA expression (**Fig. 5F** and **Supplementary Fig. 6F**) in MM cells. Furthermore,
388 using MM cells expressing an ectopic WDR82-GFP fusion protein (**Supplementary Fig.**
389 **6G**), we demonstrated that lnc-17-92 expression is essential for WDR82 occupancy at
390 the *ACACA* promoter (**Fig. 5G**). Additionally, lnc-17-92 depletion resulted in reduced
391 levels of H3K4me3 at the *ACACA* promoter (**Fig. 5H**), without globally impacting the
392 H3K4 methylation status (**Fig. 5I**).

These findings suggest lnc-17-92^{TV1} is a chromatin scaffold mediating the assembly of the MYC-WDR82 multiprotein transcriptional complex to control the expression of *ACACA* and likely other genes.

Therapeutic inhibitors of MIR17HG exert potent anti-tumor activity *in vitro* and *in vivo* in animal models of human MM.

We next explored MIR17HG as a therapeutic target, which includes both the lncRNA and miRNA factors. To develop clinically applicable inhibitors, we screened >80 fully phosphorothioated (PS), 2'-O-methoxyethyl (2'-MOE)-modified, lipid-conjugated ASOs that could either trigger RNase H–mediated degradation of MIR17HG pre-RNA (gapmeRs) or exert function via an RNase H–independent mechanism (blockmeRs)[47] (**Supplementary Fig. 7A-B**). This procedure identified an 18-mer tocopherol (T)-conjugated gapmeR G2-15b-T ("G") and an 18-mer tocopherol (T)-conjugated steric blocker SB9-19-T ("B") as both having strong anti-proliferative effects (cell growth inhibition, CGI > 50%) in a large panel of MM cell lines as well as CD138+ primary MM cells, while sparing (CGI < 50%) non-malignant cell lines (THLE-2, HK-2, HS-5 and 293T) and PBMCs from 3 healthy donors (**Supplementary Fig. 7C**).

To assess the *in vivo* anti-tumor activity of both compounds, we first used a AMO1-based plasmacytoma xenograft model in immunocompromised NOD SCID mice. Here, we observed a significant reduction of tumor growth after a treatment cycle with either G2-15b-T (tumor growth inhibition, TGI=76%) or B9-19-T (TGI=69%) (**Fig. 6A**). Analysis of tumors retrieved from mice following this treatment confirmed reduced expression of lnc-17-92 (**Fig. 6B**) and miR-17-92s (**Supplementary Fig. 7D**), as well as

modulation of lnc-17-92's targets (*ACACA*, *EPT1*, *EXT1*, *CCDC91*, *ANO6*, *FER* and *ZYG11A*) (**Fig. 6C**) and miR-17-92's target BIM (aka *BCL2L11*) (**Supplementary Fig. 7E**). We also observed reduced levels of tripalmitin (**Supplementary Fig. 7F**), a surrogate for the *de novo* lipogenesis product palmitate[48]. This demonstrates efficient uptake of G2-15b-T and B9-19-T by tumor cells *in vivo*. We observed no overt toxicity in the mice after treatment, as shown by blood cell count, clinical biochemistry (**Supplementary Tables 9-10**), and body weight analysis (not shown).

We next confirmed the significant anti-MM activity of G2-15b-T and B9-19-T in an aggressive model of diffused myeloma, in which tumor growth of MOLP8-luc+ MM cells is assessed by bioluminescence imaging (BLI). In this model, tumor growth was significantly antagonized after a treatment cycle with either G2-15b-T (TGI=84%) or B9-19-T (TGI=52%). Treatment with G2-15b-T resulted in tumor clearance in 2 out of 8 mice (25%) (**Fig. 6D**). Importantly, both inhibitors significantly prolonged animal survival (**Fig. 6E**).

Finally, we established a clinically relevant PDX-NSG mouse model by tail-vein injection of CD138+ MM cells obtained from an advanced-stage patient (PDX-NSG). In this model, tumor growth was monitored in serum samples using human kappa light chain as a surrogate. Remarkably, we observed a regression of tumor growth after a treatment cycle with G2-15b-T, whose effects were comparable to bortezomib (a positive control) (**Fig. 6F**).

DISCUSSION

MIR17HG is often amplified and/or overexpressed in human cancer and has a driver role[34,39,49]. One of its transcriptional products, pri-mir-17-92, is enzymatically digested by DROSHA into six precursor transcripts (pre-mir-17 / -18a / -19a / -20a / -19b1 / -92a) that are further processed by DICER to generate the miR-17-92 mature miRNAs (miR-17 / -18a / -19a / -20a / -19b1 / -92a). These miRNAs post-transcriptionally repress relevant tumor-suppressive mRNAs[34,39,40,49], such as the pro-apoptotic factor BIM[50]. Their impact on tumorigenesis is particularly relevant when co-expressed with MYC[34,39], as there's a well-documented interplay between miR-17-92, especially of miR-19b[51,52], and MYC transcriptional targets in maintaining cancer cell homeostasis[5,39,40]. We have previously demonstrated that these miRNAs play a relevant role in MM by forming homeostatic feed-forward loops with MYC and BIM[5]. Interestingly, our previous work also showed that depletion of mature miRNAs does not phenocopy the inhibition of MIR17HG pre-RNA, suggesting other tumor-promoting functions for this transcript[5]. An alternative mechanism to explain the oncogenic role of MIR17HG has been recently identified and involves the overload of DROSHA by an overexpressed pri-mir-17-92 in B cell lymphomas[53]. Our description in this study of the miRNA-, DROSHA- and DICER-independent function of MIR17HG, via lnc-17-92, establishes this gene as having both *short* (miR-17-92) and *long* (lnc-17-92) noncoding RNA activities, with the latter mediating tumor-promoting activity in MM and likely other cancer contexts (e.g., colorectal cancer).

We described lnc-17-92 as a specific regulator of gene expression via chromatin occupancy and interaction with MYC and WDR82. Lnc-17-92 directly reduces the

459 expression of a small subset of genes and prevents the accumulation of H3K4me3 at
460 the *ACACA* promoter. These effects are in contrast to what is observed by depleting c-
461 MYC (i.e., global effect on gene expression) or WDR82 (i.e., global effect on
462 methylation of H3K4) in cancer cells, as reported in this and other studies[44,54]. Our data
463 support the emerging paradigm whereby chromatin occupancy by transcription factors
464 like MYC may be determined through interacting with specific lncRNAs[55], in addition to
465 protein partners[26]. In a broader perspective, our observations on lnc-17-92 suggest
466 lncRNAs are key mediators of the epigenetic and transcriptional reprogramming of MM
467 cells. In this molecular scenario, while proteins act as catalytic effectors, the intrinsic
468 structural flexibility of lncRNAs makes them good modular scaffolds able to mediate
469 both protein-protein and protein-DNA interactions at specific chromatin regions.

470 We further showed that the lnc-17-92-MYC-WDR82 complex impacts tumor cell
471 metabolism by activating the *de novo* lipogenesis pathway via regulation of *ACACA*.
472 This anabolic pathway is primarily restricted to liver and adipose tissue in normal adults
473 but is reactivated in cancer cells via mechanisms yet to be fully described[38,56]. Notably,
474 MYC has been implicated in the reprogramming of tumor cell metabolism by activating
475 that pathway via *ACACA* and other genes[57]. In turn, lipogenesis has emerged as an
476 essential pathway for the onset and progression of MYC-driven cancers, which are
477 susceptible to pharmacologic inhibition of ACC1[41]. This seems particularly relevant in
478 MM, where tumor cells need to adapt their metabolic pathways to meet the high
479 bioenergetic and biosynthetic demand posed by the malignant cell growth coupled with
480 unceasing production of monoclonal immunoglobulin[58,59]. Nevertheless, we
481 acknowledge that the oncogenic roles of lnc-17-92 are likely not limited to the

transcriptional axis with *ACACA* and will require further investigation to be comprehensively elucidated.

Deletion of MIR17HG is tolerated in adult mice[60], and its haploinsufficiency is compatible with life in humans[61]. The physiological role of MIR17HG seems particularly relevant only for the hematopoietic stem cell compartment[60], which continuously renews. These observations support the development of MIR17HG as a target. Thus, for translational purposes, we developed two therapeutic ASOs that target the MIR17HG pre-RNA via different mechanisms of action (i.e., RNase H-dependent or -independent). With the recent advances in RNA medicine[62-64], the use of ASOs to therapeutically antagonize disease-driver genes is becoming increasing possible[47,65], including in MM therapy[5,66]. Our optimization of design and chemistry has helped to overcome the major obstacles to the clinical use of ASOs, such as poor bioavailability[65], while limiting off-target toxicity. The inhibitors described here bear state-of-the-art chemical modifications (2'MOE, PS-backbone, lipid conjugation) and have sufficient nucleotide length (18mer) to ensure high specificity for MIR17HG. Inhibitors of this kind have already been tested within clinical trials and a few are already FDA approved for use in different human diseases[65]. Our optimized ASOs targeting MIR17HG with demonstrated activity in 3 different murine models of human MM provide the rationale to now consider clinical application in MM.

Different questions remain open about the dual nature of MIR17HG and its therapeutic targeting. Important future directions will be to uncover how the splicing of MIR17HG is alternatively regulated to produce lnc-17-92 or miR-17-92 and to address the relative contribution of lnc-17-92 and miR-17-92 to the oncogenic activity of

MIR17HG in other cancer models. Whether the host genes of the two paralogs of miR-17-92, miR-106a-363 and miR-25-106b, also retain miRNA-independent function will be an important line of investigation.

Overall, this study establishes MIR17HG with a unique lncRNA function of facilitating protein-protein and protein-DNA interactions, mediating tumor-promoting activity with therapeutic implications.

ACKNOWLEDGEMENTS

This work is supported by NIH/NCI grants SPORE-P50CA100707, R01-CA050947, R01CA207237, P01CA155258, R01-CA178264 (N.C.M., K.C.A.); by VA Healthcare System grant No. 5I01BX001584 (N.C.M.); by the Paula and Roger Riney Foundation grant (N.C.M., K.C.A.) by NIH/NCI grants RO1CA131945, R01CA187918, P50 CA211024 and Department of Defense grants DoD PC160357 and DoD PC180582 (M.L.); by the Sheldon and Miriam Medical Research Foundation (K.C.A.); by the Italian Association for Cancer Research (AIRC) with “Special Program for Molecular Clinical Oncology–5 per mille”, 2010/15 and its Extension Program” No. 9980, 2016/18 (P.T.). E.M. is supported by a Brian D. Novis Junior Grant from the International Myeloma Foundation, by a Career Enhancement Award from Dana Farber/Harvard Cancer Center SPORE in Multiple Myeloma (SPORE-P50CA100707), by a Special Fellow grant from The Leukemia & Lymphoma Society, and by a Scholar Award from the American Society of Hematology. A.G. is supported by a Fellow grant from The Leukemia & Lymphoma Society and by a Scholar Award from the American Society of Hematology. JEH is supported by a NIH F32 fellowship (NCI 1F32CA254216-01). A.N. is supported by a grant from the Italian Association for Cancer Research (AIRC, IG24365). N.A. is supported by a grant from the Italian Association for Cancer Research (AIRC, IG24449). K.C.A. is an American Cancer Society Clinical Research Professor,

We gratefully acknowledge the members of our laboratories for technical advice and critical discussions. We thank Dr. Christina Usher (Dana-Farber Cancer Institute) for editing the manuscript and insightful comments. We thank Dr. Dirk Eick (Helmholtz-

Zentrum München, Molecular Epigenetics), Dr. Christoph Driessen (Cantonal Hospital St Gallen, St Gallen, Switzerland) and Dr. Linda Penn (Princess Margaret Cancer Centre, University Health Network, Toronto, Ontario, Canada) for providing us relevant cellular models. We thank Dr. Pierosandro Tagliaferri (Magna Graecia University, Catanzaro, Italy) for insightful discussions on the dual long and short nature of MIR17HG. We thank Dr. Benjamin Izar and Dr. Johannes Melms (Columbia University, New York, NY, USA.) for insightful discussions on CRISPR viability screen methodology. We thank the "8th Annual Miracles for Myeloma 5K Virtual Run/Walk" organizers and attendees for the fundraising in support to this research project.

AUTHOR CONTRIBUTIONS

E.M. and N.C.M. conceived and designed the research studies. E.M., M.F. and N.C.M. wrote the manuscript. M.K.S., A.A.S. and K.T. performed in silico analysis of transcriptomic data. C.F.R. performed lipidomic studies. L.W.L. performed yeast-3-hybrid experiments. J.E.H. performed RNA FISH, dual RNA FISH and Co-IF/dual RNA FISH. S.T. generated MM cells expressing CAS9. W.D.P. analyzed ChIP-seq data. S.G. designed t-ASOs. C.F., N.R., D.M. and F.S. provided support for the identification of lnc-17-92 isoforms. M.F., A.G., N.A., M.J., G.B., C.L., Y.T.T., A.N., D.C., T.H., M.A.S., P.T., R.A.Y., K.C.A., C.D.N. and M.L. contributed to the design and interpretation of key experiments. M.L. supervised lipidomic studies. C.D.N. supervised Y3H experiments.

COMPETING INTERESTS STATEMENT

N.C.M. serves on advisory boards/consultant to Takeda, BMS, Celgene, Janssen, Amgen, AbbVie, Oncopep, Karyopharm, Adaptive Biotechnology, and Novartis and holds equity ownership in Oncopep. K.C.A. serves on advisory boards to Janssen, Pfizer, Astrazeneca, Amgen, Precision Biosciences, Mana, Starton, and Raqia, and is a Scientific Founder of OncoPep and C4 Therapeutics. R.A.Y. is a founder and shareholder of Syros Pharmaceuticals, Camp4 Therapeutics, Omega Therapeutics, and Dewpoint Therapeutics. E.M., S.G. and N.C.M filed a provisional patent on MIR17HG as a target for cancer therapy. D.C. reports other support from Stemline Therapeutics, Oncopeptides, and C4 Therapeutics outside the submitted work. No potential conflicts of interest were disclosed by the other authors.

FIGURE LEGENDS

Figure 1. CRISPRi viability screens identify MIR17HG as a leading cell growth dependency in MM. A) Schematic of CRISPRi viability screens. **B**) RRA-based ranked analysis of lncRNA dependencies in the secondary screen, considering 4 MM cell lines either together or individually. The top lncRNA dependency, MIR17HG, is highlighted, along with the protein-coding genes IRF4 and MYC used as positive controls. **C**) CCK-8 proliferation assay of MM cell lines (AMO1, H929, KMS11 and KMS12BM) stably expressing KRAB-dCAS9 fusion protein and transduced with lentivectors to conditionally express anti-MIR17HG sgRNAs. CCK-8 assay was performed at indicated time points after exposure to doxycycline (0.5µg/mL). Cell proliferation is calculated compared to parental cells infected with the empty sgRNA vector and exposed to doxycycline under the same conditions. **D**) CCK-8 proliferation assay of MM cell lines (n=11) transfected with 2 different ASOs targeting the MIR17HG pre-RNA or a non-targeting ASO (NC). ASOs were used at a concentration of 25nM. Cell viability was measured 2 and 4 days after electroporation, and it is represented as % viability compared to cells transfected with NC-ASO. Data from 1 out of 3 independent experiments is shown in panel D and E. Data present mean ± s.d.in D and E. *p<0.05 by Student's t test.

Figure 2. MIR17HG-derived lnc-17-92 mediates cell growth dependency in a miRNA- and DROSHA- independent manner. A) Overview of MIR17HG locus, including both lncRNA (lnc-17-92) and miRNA (miR-17-92)-derived transcripts. **B**) Single molecule RNA FISH analysis of subcellular localization of lnc-17-92 in AMO1.

589 Cell nuclei are stained by DAPI. **C**) Prognostic significance (PFS and OS) of high lnc-
590 17-92 expression (top quartile) in 3 large cohorts of MM patients. **D**) CCK-8 proliferation
591 assay in AMO1 and H929 cells stably transduced with either a lentivector carrying pri-
592 mir-17-92 (pri-miR) or a lentiviral vector carrying GFP as a control, and transfected with
593 2 different ASOs targeting the 5'end (5'-ASO) of MIR17HG pre-RNA or a scrambled
594 control (NC). Effects on cell proliferation were assessed 48h after transfection. **E**) CCK-
595 8 proliferation assay of DROSHA WT or KO AMO1 and H929 exposed to ASO1 (1μM
596 for AMO1 and 2.5μM for H929) for 6 days. Western blot analysis of DROSHA
597 expression in WT and KO cells. Vinculin was used as a protein-loading control. **F**)
598 Effects of lnc-17-92 depletion in a matrigel-based $AMO1^{DR-KO}$ xenograft in NOD SCID
599 mice. Tumor growth of $AMO1^{DR-KO}$ with (ASO-1) or without (NC) lnc-17-92 depletion. **G**)
600 Survival analysis of tumor-injected mice. *indicates $p<0.05$, *ns* indicates $p>0.05$ after
601 Student's t test.
602
603 **Figure 3. Lnc-17-92 forms a transcriptional axis with *ACACA* to promote**
604 **proliferation and survival of MM cells. A**) Transcriptomic analysis after lnc-17-92
605 depletion in MM cell lines that have either DROSHA WT (AMO1, H929) or KO ($AMO1^{DR-}$
606 ^{KO}). Venn diagram of commonly downregulated genes (adj $p<0.05$; log2FC<-1). Cells
607 were exposed to ASO1 for 24h. **B**) qRT-PCR analysis of lnc-17-92 targets in CD138+
608 cells from 3 MM patients exposed to ASO1 for 24h. The results shown are average
609 mRNA expression levels after normalization with GAPDH and ΔΔCt calculations. RNA
610 level in cells exposed to NC (vehicle) were set as an internal reference. **C**) Correlation
611 analysis between lnc-17-92 targets (mRNA) and lnc-17-92 in CD138+ MM patient cells

612 from 2 large RNA-seq cohorts (DFCI/IFM, n=360; MMRF/CoMMpass, n=720).
613 Spearman *r* obtained in DFCI/IFM (*x* axis) and MMRF/CoMMpass (*y* axis) dataset.
614 Dotted red lines indicate *r*=0.3. Individual correlation plots are shown below. **D**) GLuc/
615 SEAP dual reporter assay showing reduced activity of *ACACA*, *ANO6*, *CCDC91*, *EPT1*,
616 *EXT1*, *FER* and *KIAA1109* promoter activity after lnc-17-92 knockdown using ASO1.
617 The reporter vectors were co-transfected into 293T cells with either ASO1 or control
618 ASO. Cells were harvested for the luciferase activity assay 48h after transfection.
619 Results are shown as % of normalized Gluc activity in ASO1-transfected cells compared
620 to control. **E**) ChIRP-qPCR analysis showing effective amplification of *ACACA* promoter
621 in chromatin purified using two lnc-17-92 antisense probe sets (ps1 and ps2), compared
622 to chromatin purified using LacZ antisense probes (negative control). **F**) (left) Snapshot
623 obtained by dual RNA-FISH analysis of *ACACA* pre-mRNA (green) and lnc-17-92
624 (purple) in a representative AMO1 cell; (right) box plot showing the distance (nm) of
625 *ACACA* pre-RNA spots to the nearest lnc-17-92 spots (n=57) or to the nearest random
626 spots (160). 300nm was used as a cut-off determining proximity. **G**) CCK-8 proliferation
627 assay in 5 MM cells lines after transfection with siRNAs against lnc-17-92 targets. Two
628 siRNAs were used for each target, plus a scramble siRNA (NC) as a control. Cell
629 viability was measured at the indicated time point and it is represented as % of NC-
630 transfected cells. *indicates $p<0.05$ after Student's t test in panels B, D, and G, or after
631 Fisher Exact Test in E and F.
632
633 **Figure 4. Lnc-17-92 directly interacts with c-MYC and promotes its occupancy at**
634 **the *ACACA* promoter. A**) Western blot analysis of MYC in RPPD material precipitated

with control RNA or lnc-17-92^{TV1} or lnc-17-92^{TV2}. 5% input is used as a reference. **B**) qRT-PCR analysis of lnc-17-92 (detecting lnc-17-92^{TV1}) in RIP material precipitated using an anti-MYC antibody (α-MYC) or IgG control. LncRNA PVT1 is used as a positive control for its role as MYC interactor. **C**) RNA Y3H using MYC as hybrid protein 2 and, as hybrid RNAs, a negative control RNA (-) or lnc-17-92^{TV1} or lnc-17-92^{TV2}. **D**) ChIP-qPCR analysis of MYC occupancy at the *ACACA* promoter in AMO1, H929 and U266^{MYC+} exposed for 24h to ASO1 or NC (vehicle). MYC occupancy at *ACACA* promoter is calculated as % of input chromatin. Below each histogram plot is the western blot analysis of MYC from paired samples. GAPDH or α-tubulin were used as protein loading controls. **E**) qRT-PCR analysis of *ACACA* mRNA in P493-6 cells exposed for 2 days to either doxycycline or DMSO to knockdown MYC, and then exposed for 2 additional days to either ASO1 or vehicle (NC) to deplete lnc-17-92. *ACACA* expression levels in cells exposed to NC were set as an internal reference. *p < 0.05, Student's t test.

Figure 5. Lnc-17-92 mediates the assembly of a MYC-WDR82 transcriptional complex, leading to transcriptional and epigenetic activation of *ACACA*. A) Schematic of integrated BioID and Co-IP/MS assays to explore the MYC-protein interacting network in the presence or absence of lnc-17-92 depletion. **B**) Western blot analysis of WDR82 in RPPD material precipitated with lnc-17-92^{TV1} or lnc-17-92^{TV2} or with control RNA. 5% input is used as a reference. **C**) RNA Y3H using WDR82 as hybrid protein 2 and, as hybrid RNAs, either a negative control RNA (-) or lnc-17-92^{TV1} or lnc-17-92^{TV2}. Red arrows indicate yeast colony growth. **D**) ChIP-qPCR analysis of

H3K4me3 occupancy at *ACACA* promoter after silencing of WDR82 with a siRNA pool (n-4) in H929 (24h time point). Data are represented as % of input chromatin. **E**) ChIP-qPCR analysis of MYC occupancy at the *ACACA* promoter after silencing of WDR82 with a siRNA pool (n-4) (24h time point). Data are represented as % of input chromatin. **F**) qRT-PCR analysis of *ACACA* mRNA after silencing of WDR82 with a siRNA pool (n-4) (48h time point). Raw Ct values were normalized to GAPDH mRNA and expressed as ΔΔCt values calculated using the comparative cross threshold method. *ACACA* expression levels in cells transfected with NC were set as an internal reference. **G**) ChIP-qPCR analysis of WDR82-GFP occupancy at the *ACACA* promoter in AMO1 exposed for 24h to gymnotic ASO1. Data are represented as % of input chromatin. Western blot analysis of WDR82-GFP from paired samples. α-tubulin was used as the protein loading control. **H**) ChIP-qPCR analysis of H3K4me3 occupancy at the *ACACA* promoter in AMO1 and H929 exposed for 24h to gymnotic ASO1. Data are represented as % of input chromatin. **I**) Western blot analysis of H3, H3H3K4me1, H3H3K4me2, and H3H3K4me3 in AMO1 and H929 exposed for 24h to gymnotic ASO1. Lamin A/C was used as the protein loading controls (nuclear lysates). *$p < 0.05$, Student's t test.

Figure 6. Therapeutic inhibitors of MIR17HG exert potent anti-tumor activity *in vitro* and *in vivo* in animal models of human MM. A) Subcutaneous *in vivo* tumor growth of AMO1 cells in NOD SCID mice, 21 days after treatment with G2-15b*-TO (G; n=5) or B9-19-TO (B; n=5) or vehicle (NC; n=5). **B-C**) qRT-PCR analysis of lnc-17-92 (C) and lnc-17-92 targets (D) in AMO1 xenografts, retrieved from animals treated with G2-15b*-TO (G; n=1) or B9-19-TO (B; n=1) or vehicle (NC; n=1) as a control. Raw Ct

values were normalized to *ACTB* mRNA and expressed as ΔΔCt values calculated using the comparative cross threshold method. Expression levels in NC were set as an internal reference. **D**) BLI-based measurement of *in vivo* tumor growth of MOLP8-luc+ in NSG mice, after treatment with G2-15b*-TO (G; n=8) or B9-19-TO (B; n=6) or vehicle (NC; n=11). On the top, a scatter plot showing the analysis of bioluminescence intensity. Red bars indicate median value. Bioluminescence was measured at the end of the treatment cycle (day 15). Below, image acquisition. Mice removed from the study due to failed I.V. injection of tumor cells are covered by a black rectangle. **E**) Survival analysis from experiment in panel E. **F**) Human Kappa light chain ELISA-based measurement of *in vivo* tumor growth of MM patient cells in NSG mice (PDX-NSG), after treatment with G2-15b*-TO (G; n=2), bortezomib (BTZ; n=2) or vehicle (NC; n=3). Black arrows indicate treatments. *indicates $p<0.05$; **means $p<0.01$; ***means $p<0.001$.

693 REFERENCES

694 1. Gulla A, Anderson KC. Multiple myeloma: the (r)evolution of current therapy and a
695 glance into future. *Haematologica*. 2020.
696 2. Morelli E, Gulla A, Rocca R, et al. The Non-Coding RNA Landscape of Plasma Cell
697 Dyscrasias. *Cancers (Basel)*. 2020;12(2).
698 3. Pichiorri F, Suh SS, Rocci A, et al. Downregulation of p53-inducible microRNAs 192, 194,
699 and 215 Impairs the p53/MDM2 Autoregulatory Loop in Multiple Myeloma Development.
700 *Cancer Cell*. 2016;30(2):349-351.
701 4. Amodio N, Stamato MA, Juli G, et al. Drugging the lncRNA MALAT1 via LNA gapmeR ASO
702 inhibits gene expression of proteasome subunits and triggers anti-multiple myeloma activity.
703 *Leukemia*. 2018;32(9):1948-1957.
704 5. Morelli E, Biamonte L, Federico C, et al. Therapeutic vulnerability of multiple myeloma
705 to MIR17PTi, a first-in-class inhibitor of pri-miR-17-92. *Blood*. 2018;132(10):1050-1063.
706 6. Hu Y, Lin J, Fang H, et al. Targeting the MALAT1/PARP1/LIG3 complex induces DNA
707 damage and apoptosis in multiple myeloma. *Leukemia*. 2018;32(10):2250-2262.
708 7. Morelli E, Leone E, Cantafio ME, et al. Selective targeting of IRF4 by synthetic microRNA-
709 125b-5p mimics induces anti-multiple myeloma activity in vitro and in vivo. *Leukemia*.
710 2015;29(11):2173-2183.
711 8. Leone E, Morelli E, Di Martino MT, et al. Targeting miR-21 inhibits in vitro and in vivo
712 multiple myeloma cell growth. *Clin Cancer Res*. 2013;19(8):2096-2106.
713 9. Wang Z, Yang B, Zhang M, et al. lncRNA Epigenetic Landscape Analysis Identifies EPIC1
714 as an Oncogenic lncRNA that Interacts with MYC and Promotes Cell-Cycle Progression in Cancer.
715 *Cancer Cell*. 2018;33(4):706-720 e709.
716 10. Hon CC, Ramilowski JA, Harshbarger J, et al. An atlas of human long non-coding RNAs
717 with accurate 5' ends. *Nature*. 2017;543(7644):199-204.
718 11. Ulitsky I, Bartel DP. lincRNAs: genomics, evolution, and mechanisms. *Cell*.
719 2013;154(1):26-46.
720 12. Lu Y, Zhao X, Liu Q, et al. lncRNA MIR100HG-derived miR-100 and miR-125b mediate
721 cetuximab resistance via Wnt/beta-catenin signaling. *Nat Med*. 2017;23(11):1331-1341.
722 13. Tseng YY, Moriarity BS, Gong W, et al. PVT1 dependence in cancer with MYC copy-
723 number increase. *Nature*. 2014;512(7512):82-86.
724 14. Gutschner T, Diederichs S. The hallmarks of cancer: a long non-coding RNA point of
725 view. *RNA Biol*. 2012;9(6):703-719.
726 15. Samur MK, Minvielle S, Gulla A, et al. Long intergenic non-coding RNAs have an
727 independent impact on survival in multiple myeloma. *Leukemia*. 2018;32(12):2626-2635.
728 16. Carrasco-Leon A, Ezponda T, Meydan C, et al. Characterization of complete lncRNAs
729 transcriptome reveals the functional and clinical impact of lncRNAs in multiple myeloma.
730 *Leukemia*. 2021.
731 17. Ronchetti D, Agnelli L, Taiana E, et al. Distinct lncRNA transcriptional fingerprints
732 characterize progressive stages of multiple myeloma. *Oncotarget*. 2016;7(12):14814-14830.
733 18. Liu SJ, Horlbeck MA, Cho SW, et al. CRISPRi-based genome-scale identification of
734 functional long noncoding RNA loci in human cells. *Science*. 2017;355(6320).

19. Morelli E, Gulla A, Amodio N, et al. CRISPR Interference (CRISPRi) and CRISPR Activation (CRISPRa) to Explore the Oncogenic lncRNA Network. *Methods Mol Biol*. 2021;2348:189-204.
20. Taiana E, Favasuli V, Ronchetti D, et al. In Vitro Silencing of lncRNAs Using LNA GapmeRs. *Methods Mol Biol*. 2021;2348:157-166.
21. Shaffer SM, Wu MT, Levesque MJ, Raj A. Turbo FISH: a method for rapid single molecule RNA FISH. *PLoS One*. 2013;8(9):e75120.
22. Raj A, van den Bogaard P, Rifkin SA, van Oudenaarden A, Tyagi S. Imaging individual mRNA molecules using multiple singly labeled probes. *Nat Methods*. 2008;5(10):877-879.
23. Chu C, Quinn J, Chang HY. Chromatin isolation by RNA purification (ChIRP). *J Vis Exp*. 2012(61).
24. Zadra G, Ribeiro CF, Chetta P, et al. Inhibition of de novo lipogenesis targets androgen receptor signaling in castration-resistant prostate cancer. *Proc Natl Acad Sci U S A*. 2019;116(2):631-640.
25. Fulciniti M, Lin CY, Samur MK, et al. Non-overlapping Control of Transcriptome by Promoter- and Super-Enhancer-Associated Dependencies in Multiple Myeloma. *Cell Rep*. 2018;25(13):3693-3705 e3696.
26. Kalkat M, Resetca D, Lourenco C, et al. MYC Protein Interactome Profiling Reveals Functionally Distinct Regions that Cooperate to Drive Tumorigenesis. *Mol Cell*. 2018;72(5):836-848 e837.
27. Li W, Xu H, Xiao T, et al. MAGeCK enables robust identification of essential genes from genome-scale CRISPR/Cas9 knockout screens. *Genome Biol*. 2014;15(12):554.
28. Shaffer AL, Emre NC, Lamy L, et al. IRF4 addiction in multiple myeloma. *Nature*. 2008;454(7201):226-231.
29. Chesi M, Robbiani DF, Sebag M, et al. AID-dependent activation of a MYC transgene induces multiple myeloma in a conditional mouse model of post-germinal center malignancies. *Cancer Cell*. 2008;13(2):167-180.
30. Jovanovic KK, Escure G, Demonchy J, et al. Deregulation and Targeting of TP53 Pathway in Multiple Myeloma. *Front Oncol*. 2018;8:665.
31. Tessoulin B, Moreau-Aubry A, Descamps G, et al. Whole-exon sequencing of human myeloma cell lines shows mutations related to myeloma patients at relapse with major hits in the DNA regulation and repair pathways. *J Hematol Oncol*. 2018;11(1):137.
32. Lai F, Damle SS, Ling KK, Rigo F. Directed RNase H Cleavage of Nascent Transcripts Causes Transcription Termination. *Mol Cell*. 2020;77(5):1032-1043 e1034.
33. Lee JS, Mendell JT. Antisense-Mediated Transcript Knockdown Triggers Premature Transcription Termination. *Mol Cell*. 2020;77(5):1044-1054 e1043.
34. He L, Thomson JM, Hemann MT, et al. A microRNA polycistron as a potential human oncogene. *Nature*. 2005;435(7043):828-833.
35. Ota A, Tagawa H, Karnan S, et al. Identification and characterization of a novel gene, C13orf25, as a target for 13q31-q32 amplification in malignant lymphoma. *Cancer Res*. 2004;64(9):3087-3095.
36. Bartel DP. MicroRNAs: genomics, biogenesis, mechanism, and function. *Cell*. 2004;116(2):281-297.
37. Cummins JM, He Y, Leary RJ, et al. The colorectal microRNAome. *Proc Natl Acad Sci U S A*. 2006;103(10):3687-3692.

38. Rohrig F, Schulze A. The multifaceted roles of fatty acid synthesis in cancer. *Nat Rev Cancer*. 2016;16(11):732-749.
39. Li Y, Choi PS, Casey SC, Dill DL, Felsher DW. MYC through miR-17-92 suppresses specific target genes to maintain survival, autonomous proliferation, and a neoplastic state. *Cancer Cell*. 2014;26(2):262-272.
40. Izreig S, Samborska B, Johnson RM, et al. The miR-17 approximately 92 microRNA Cluster Is a Global Regulator of Tumor Metabolism. *Cell Rep*. 2016;16(7):1915-1928.
41. Gouw AM, Margulis K, Liu NS, et al. The MYC Oncogene Cooperates with Sterol-Regulated Element-Binding Protein to Regulate Lipogenesis Essential for Neoplastic Growth. *Cell Metab*. 2019;30(3):556-572 e555.
42. Hook B, Bernstein D, Zhang B, Wickens M. RNA-protein interactions in the yeast three-hybrid system: affinity, sensitivity, and enhanced library screening. *RNA*. 2005;11(2):227-233.
43. Schuhmacher M, Staege MS, Pajic A, et al. Control of cell growth by c-Myc in the absence of cell division. *Curr Biol*. 1999;9(21):1255-1258.
44. Lee JH, Skalnik DG. Wdr82 is a C-terminal domain-binding protein that recruits the Setd1A Histone H3-Lys4 methyltransferase complex to transcription start sites of transcribed human genes. *Mol Cell Biol*. 2008;28(2):609-618.
45. Beurton F, Stempor P, Caron M, et al. Physical and functional interaction between SET1/COMPASS complex component CFP-1 and a Sin3S HDAC complex in C. elegans. *Nucleic Acids Res*. 2019;47(21):11164-11180.
46. Amente S, Lania L, Majello B. Epigenetic reprogramming of Myc target genes. *Am J Cancer Res*. 2011;1(3):413-418.
47. Puttaraju M, Jackson M, Klein S, et al. Systematic screening identifies therapeutic antisense oligonucleotides for Hutchinson-Gilford progeria syndrome. *Nat Med*. 2021.
48. Falchook G, Infante J, Arkenau HT, et al. First-in-human study of the safety, pharmacokinetics, and pharmacodynamics of first-in-class fatty acid synthase inhibitor TVB-2640 alone and with a taxane in advanced tumors. *EClinicalMedicine*. 2021;34:100797.
49. Mogilyansky E, Rigoutsos I. The miR-17/92 cluster: a comprehensive update on its genomics, genetics, functions and increasingly important and numerous roles in health and disease. *Cell Death Differ*. 2013;20(12):1603-1614.
50. Labi V, Peng S, Klironomos F, et al. Context-specific regulation of cell survival by a miRNA-controlled BIM rheostat. *Genes Dev*. 2019;33(23-24):1673-1687.
51. Olive V, Bennett MJ, Walker JC, et al. miR-19 is a key oncogenic component of mir-17-92. *Genes Dev*. 2009;23(24):2839-2849.
52. Olive V, Sabio E, Bennett MJ, et al. A component of the mir-17-92 polycistronic oncomir promotes oncogene-dependent apoptosis. *Elife*. 2013;2:e00822.
53. Donayo AO, Johnson RM, Tseng HW, et al. Oncogenic Biogenesis of pri-miR-17 approximately 92 Reveals Hierarchy and Competition among Polycistronic MicroRNAs. *Mol Cell*. 2019;75(2):340-356 e310.
54. Lin CY, Loven J, Rahl PB, et al. Transcriptional amplification in tumor cells with elevated c-Myc. *Cell*. 2012;151(1):56-67.
55. Zhang B, Lu HY, Xia YH, Jiang AG, Lv YX. Long non-coding RNA EPIC1 promotes human lung cancer cell growth. *Biochem Biophys Res Commun*. 2018;503(3):1342-1348.

822 56. Beloribi-Djefaflia S, Vasseur S, Guillaumond F. Lipid metabolic reprogramming in cancer
823 cells. *Oncogenesis*. 2016;5:e189.
824 57. Stine ZE, Walton ZE, Altman BJ, Hsieh AL, Dang CV. MYC, Metabolism, and Cancer.
825 *Cancer Discov*. 2015;5(10):1024-1039.
826 58. Masarwi M, DeSchiffart A, Ham J, Reagan MR. Multiple Myeloma and Fatty Acid
827 Metabolism. *JBMR Plus*. 2019;3(3):e10173.
828 59. El Arfani C, De Veirman K, Maes K, De Bruyne E, Menu E. Metabolic Features of Multiple
829 Myeloma. *Int J Mol Sci*. 2018;19(4).
830 60. Brinkmann K, Ng AP, de Graaf CA, et al. miR17~92 restrains pro-apoptotic BIM to ensure
831 survival of haematopoietic stem and progenitor cells. *Cell Death Differ*. 2020;27(5):1475-1488.
832 61. Sirchia F, Di Gregorio E, Restagno G, et al. A case of Feingold type 2 syndrome associated
833 with keratoconus refines keratoconus type 7 locus on chromosome 13q. *Eur J Med Genet*.
834 2017;60(4):224-227.
835 62. Sullenger BA, Nair S. From the RNA world to the clinic. *Science*. 2016;352(6292):1417-
836 1420.
837 63. Crooke ST, Witztum JL, Bennett CF, Baker BF. RNA-Targeted Therapeutics. *Cell Metab*.
838 2018;27(4):714-739.
839 64. Damase TR, Sukhovershin R, Boada C, Taraballi F, Pettigrew RI, Cooke JP. The Limitless
840 Future of RNA Therapeutics. *Front Bioeng Biotechnol*. 2021;9:628137.
841 65. Dhuri K, Bechtold C, Quijano E, et al. Antisense Oligonucleotides: An Emerging Area in
842 Drug Discovery and Development. *J Clin Med*. 2020;9(6).
843 66. Mondala PK, Vora AA, Zhou T, et al. Selective antisense oligonucleotide inhibition of
844 human IRF4 prevents malignant myeloma regeneration via cell cycle disruption. *Cell Stem Cell*.
845 2021;28(4):623-636 e629.

Figure 1

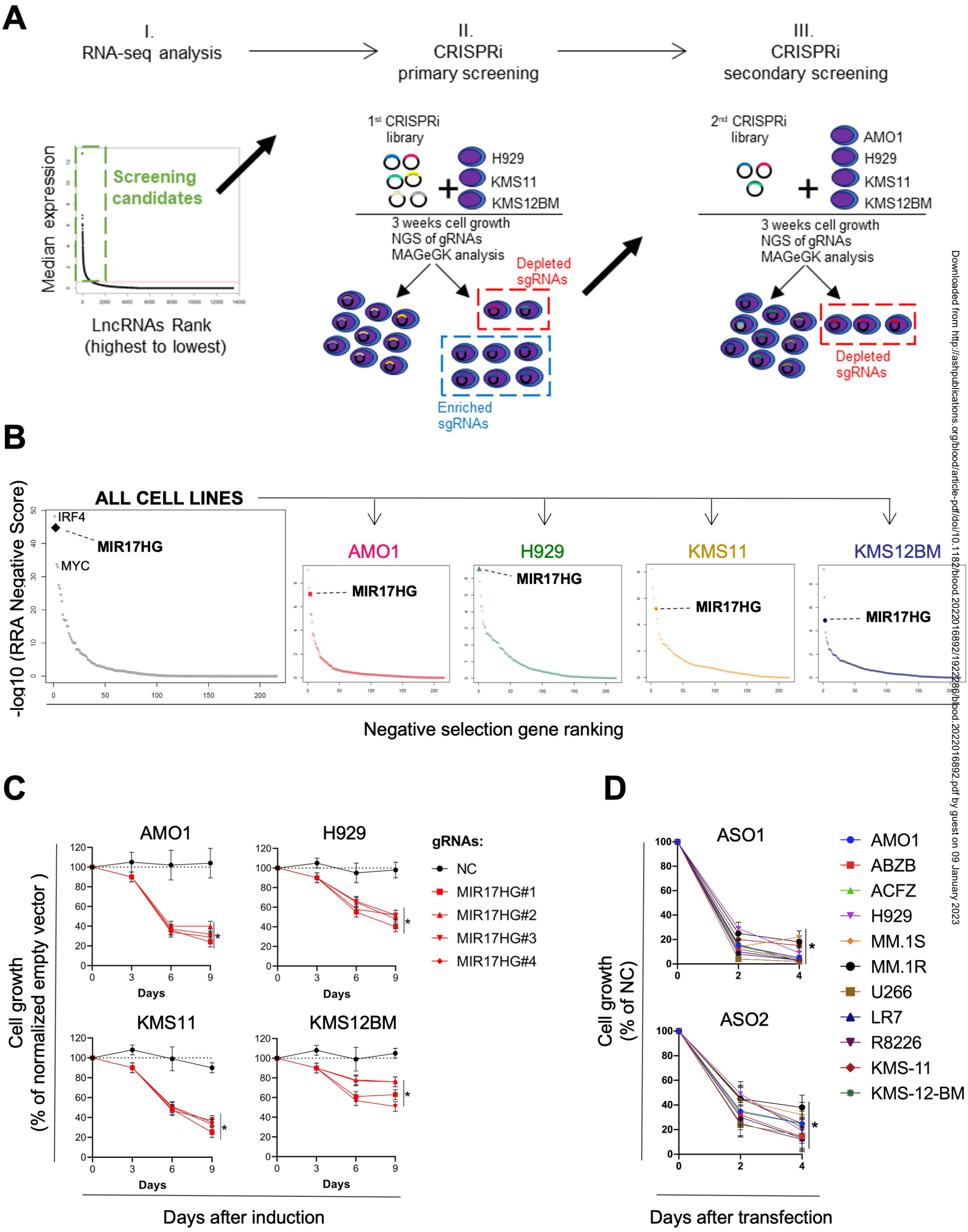

Figure 2

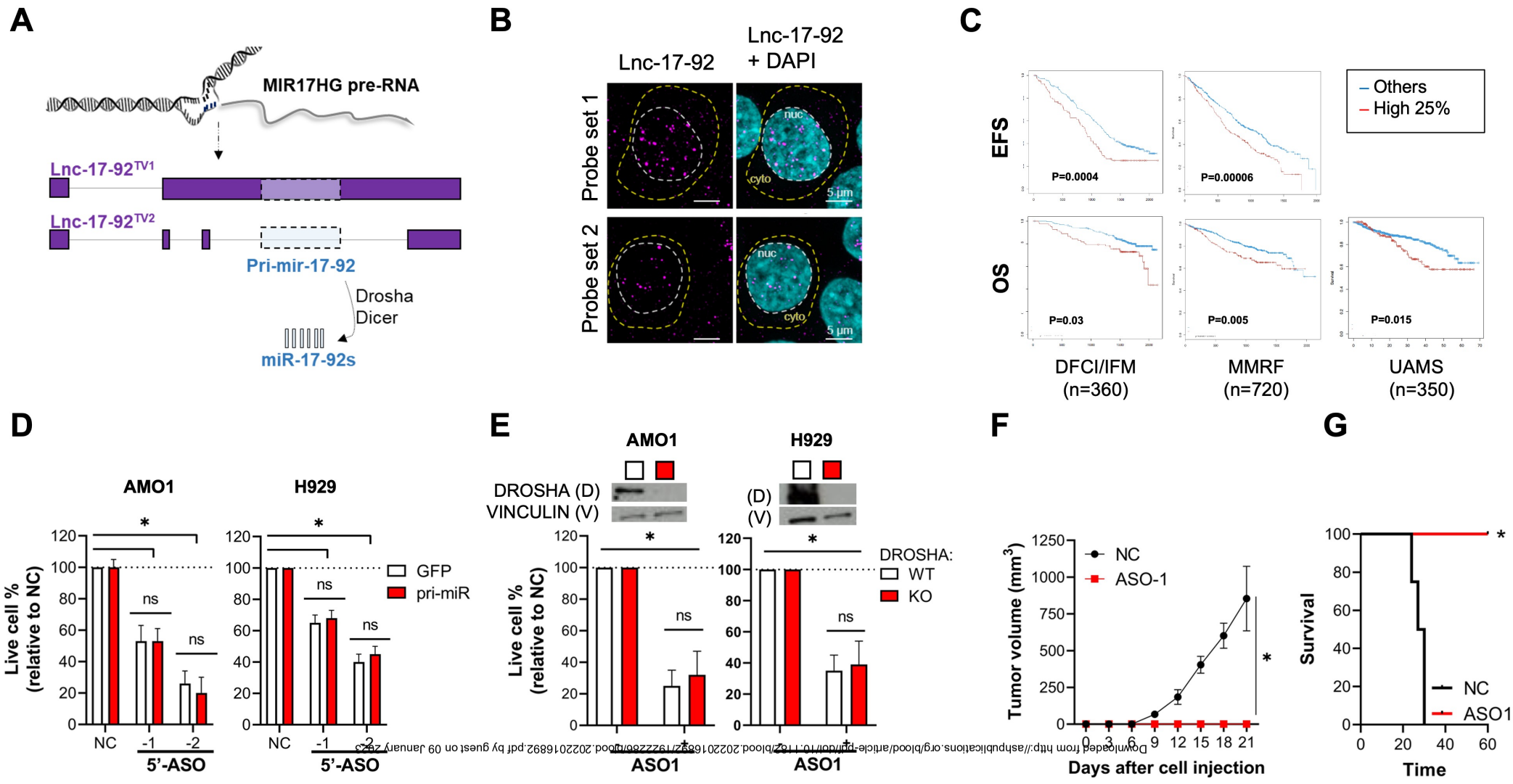

Figure 3

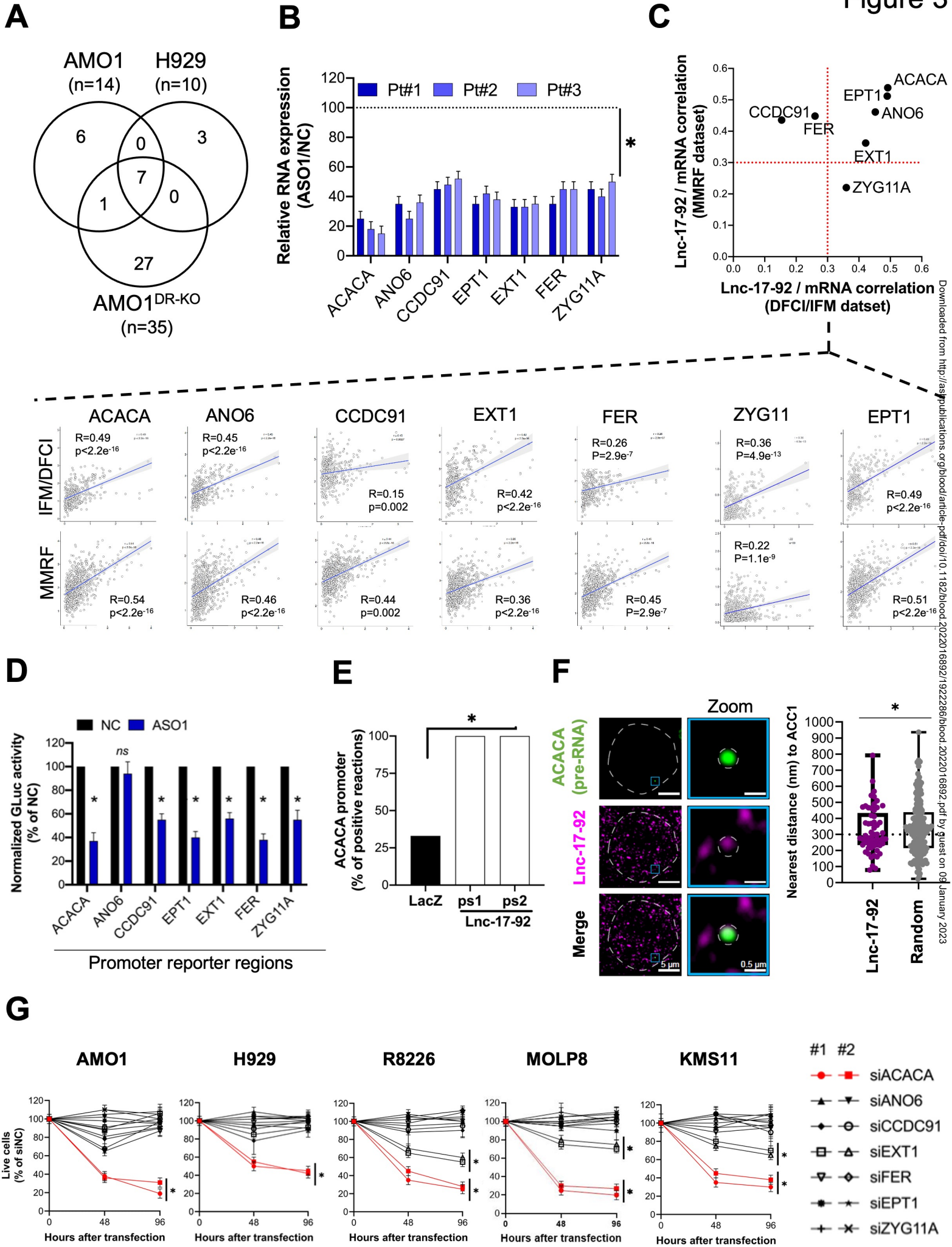

Figure 4

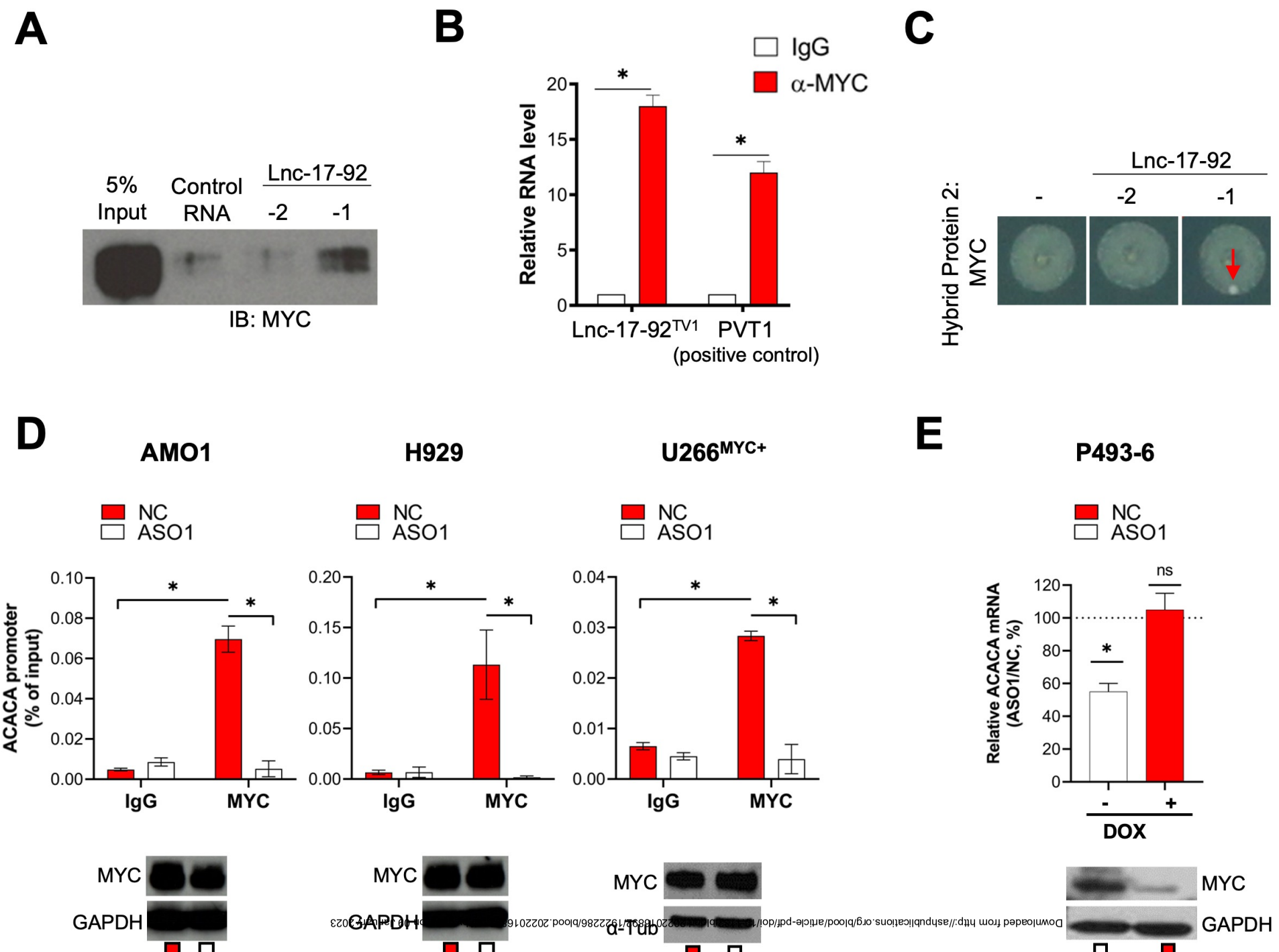

Figure 5

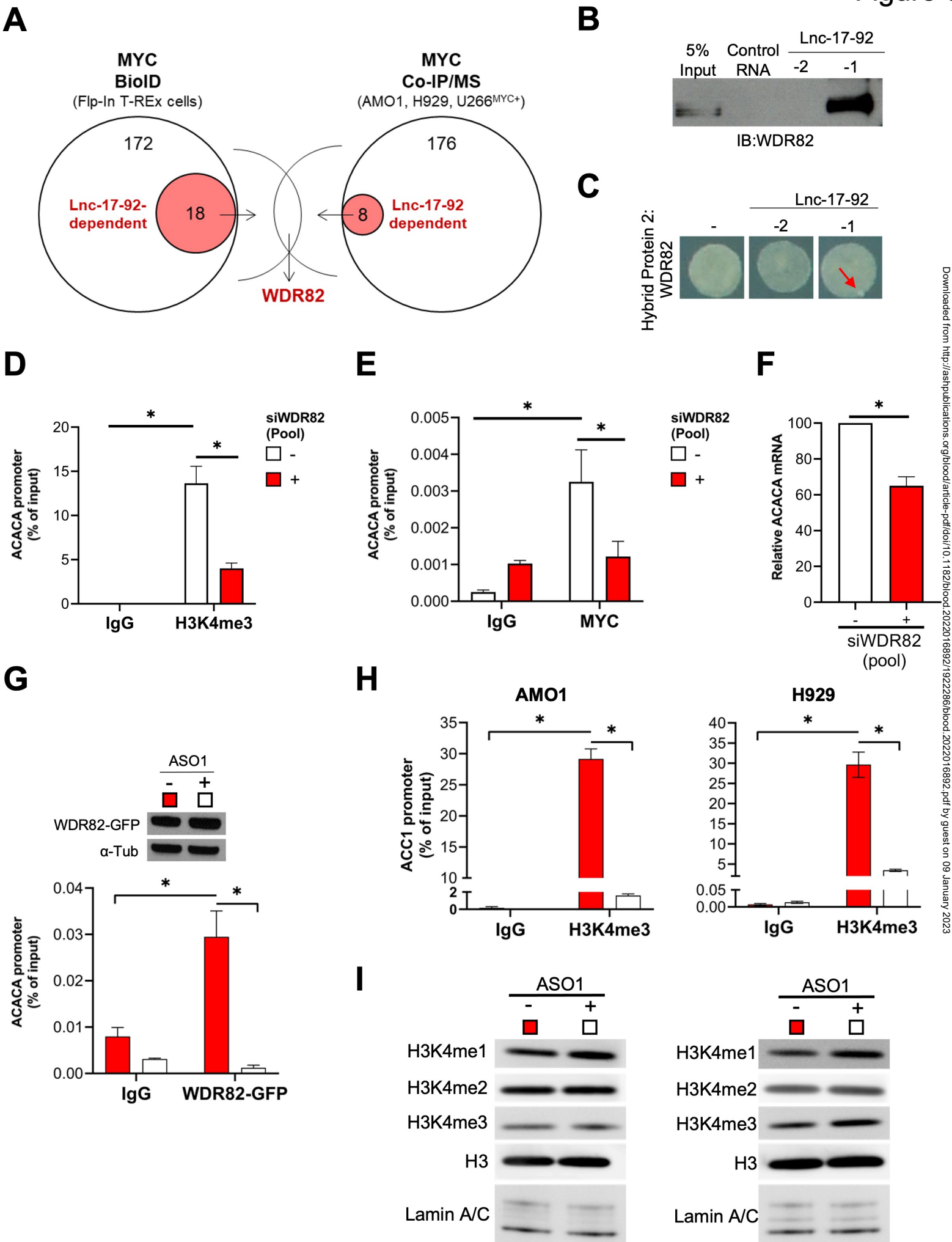

Figure 6